Investigations on Instabilities of Electric Arcs

K. Ragaller

Brown Boveri Research Center, CH-5401 Baden, Switzerland

(Z. Naturforsch. **29 a**, 556–567 [1974]; received January 16, 1974)

A general formalism is derived, that allows the evaluation of magnetic instabilities of all types of electric arc.

It is shown that a stability criterion exists which is determined by the interaction between the magnetic forces, the frictional force and the so-called isotherm movement. This criterion can be expressed in terms of a dimensionless parameter Mk: when Mk is smaller than a critical value Mk_{cr}, then the arc is absolutely stable, when $Mk = Mk_{cr}$ a stationary, deflected condition arises, and when $Mk > Mk_{cr}$ the arc is unstable. Depending on the magnitude of the growth rate however, a convective stabilisation, caused by an axial flow component, can result.

The results of the theory are applied to a variety of technically interesting arcs, such as axially blown arcs, arcs in gaps and transversely blown arcs.

1. Introduction

Electric arcs display unstable behaviour under very different conditions. The instability is seen as a deformation of the arc column which increases with time. Experience has shown that this is especially true for high current arcs ($I > 1$ kA) and for arcs which interact with gas flows (e. g. transversely blown electric arcs). It is exactly these types of arc however which are of greatest practical interest especially in circuit breakers.

Since the appearance of an instability can completely alter the behaviour of the electric arc, it is of the greatest importance to be able to make predictions concerning stable behaviour and to know the determining influences. Only then is it possible to take appropriate measures to produce stabilisation or to exploit the instability in a predictable manner.

The first theoretical investigations on the appearance of instabilities in an electric arc were carried out by Mentel [1]. He was able to show that the instability of a wall stabilised arc begins with a stationary helically deflected arc, which is represented in the stability theory by a growth rate zero. On one side of this case of neutral stability only stable arcs are produced, while on the other they are unstable. The latter, however, were not included in the description. In [2] Mentel's results were transformed into a convenient dimensionless form.

The most important factors which influence the stationary deflected arc are a driving force, in the form of the self induced magnetic field, a stabilising force, in the form of the asymmetrical heating and cooling (isotherm movement), as well as the frictional force on the flow.

Another case of instability was investigated in [3], a high current, convection stabilised electric arc. In this case also a helical instability was seen to appear on one side of a critical boundary. Theoretical analysis showed that neither the isotherm movement, nor the friction in the gas flow were of importance. The stability criterion was found to depend on the inertial forces in the flow and on the convective stabilisation. For this reason no stable deflected condition existed for this case.

The purpose of this investigation is to find an unified representation for the stability of electric arcs which takes account of the two special cases mentioned and which, in addition, is applicable to other types of arc.

2. Description of the Method

2.1. Undisturbed Initial Condition

Calculations are carried out within the framework of linear stability theory. The initial condition under investigation is represented as the physical quantity A^0, upon which are superimposed small perturbations A^*, which are then observed in order to see whether they grow or decay.

The initial condition, A^0, of the electric arc is characterised by a cylindrical plasma column with (firstly) a circular cross-section of radius R. The boundary of this arc, represented by $r = R$, is, by definition, an isotherm. Depending on the electric arc type, i. e. upon on the boundary conditions, the initial condition is associated with a temperature distribution T^0, and a flow field $\boldsymbol{v}^0$.

The analysis is limited to those cases where the axial component of the flow velocity is zero or constant. In the latter case the equations are transformed to a system moving with the arc in which the stability of the arc is followed.

Examples of such initial conditions are:

- wall stabilised arc
- axially blown arc
- transversely blown arc
- non-stationary free burning arc (where it is understood that with the growth of the arc column the non-stationarity grows slowly by comparison with the instability).

2.2. *Short Summary of the General Stability Theory* [4]

To begin with all perturbations are expanded into a complete set of normal modes.

$$A^*(r, z, \theta, t) = \sum_{m=-\infty}^{\infty} \int_{-\infty}^{\infty} A^*_{m,k}(r, t) \exp\{i(k z + m \theta)\} \cdot \mathrm{d}k . \quad (1)$$

The temporal dependence is represented by an exponential term

$$A^*_{mk}(r, t) = A^*_{mk}(r)\, e^{\lambda_k t} . \quad (2)$$

The time dependent partial differential equations (Mass momentum and energy conservation) are transformed, together with the expressions (2), into a time independent differential equation containing the parameter λ_k. In order that the boundary condition be fulfilled it is found that λ_k takes characteristic values which are functions of the parameters of the system X_i (e. g. pressure, current, arc radius etc.).

$$\lambda_k = \lambda_k(X_1, X_2, \ldots, X_j) . \quad (3)$$

The factor which therefore determines the stability is the sign of the real part of λ_k.

$$\mathrm{Re}\{\lambda_k\} = 0 \quad (4)$$

which, when substituted in (3) gives the so-called stability boundary for the mode in question.

$$X_1 = X_1(X_2 \ldots X_j) . \quad (5)$$

When, in an experimental situation, the various parameters are varied, the mode which appears is that which first satisfies the neutral stability conditions.

2.3. *Introduction of Integral Values which Simplify the Description of the Disturbed Electric Arc*

In the derivation of a stability theory suitable for the electric arc, the following guide lines should be followed.

(a) Introduction of appropriate and clearly significant integral values which should, if possible, be measurable.

(b) Demonstration of the cooperative effects of the integral values on derivation of the stability criterion (5).

2.3.1. The Arc Axis

Following these lines the position of the arc axis can be derived from the perturbation of the temperature $T^*_{m,k}$ using (3).

The position of the arc axis is defined by the position of the boundary isotherm in the plane $z =$ const (see Figure 1).

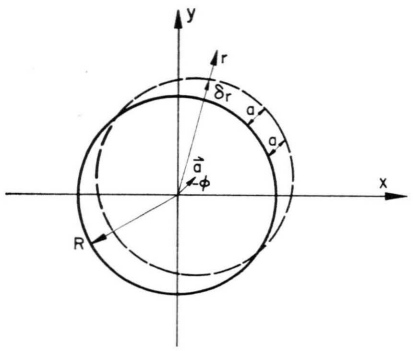

Fig. 1. Boundary isotherm of the stable (full curve) and the deflected (dashed curve) arc in planes z=const.

Only $m = 1$ instabilities are investigated [see Eq. (1)] since experiment has shown these to be the most unstable.

From Eq. (1) is then derived a linear approximation for the shift of the boundary isotherm in a radial direction.

$$\delta r(z, \theta) = - \frac{T^*(R)}{(\partial T^0/\partial r)_R} \cos(\theta + k z) . \quad (6)$$

In planes $z = \mathrm{const} = \varphi/k$ the above expression represents a shift of the undisturbed boundary isotherm in the direction $\boldsymbol{e}_1 = (\cos\varphi, \sin\varphi)$ by the amount $a = -[T^*(R)/(\partial T^0/\partial r)_R]$ which is the same at every point on the boundary.

The arc axis, which is here defined as lying at the centre of the circular boundary isotherm, will cor-

respondingly be shifted by an amount a and it follows that:

$$x = a_x \cos\varphi\,,$$
$$y = a_y \sin\varphi\,,$$
$$z = b\,\varphi\,. \tag{7}$$

This corresponds to a helically formed deformation in which b is the reduced pitch of the helix

$$b = 1/k = \lambda/2\,\pi\,. \tag{8}$$

Figure 2 shows an example of such a deformed arc column. Corresponding to the superposition of

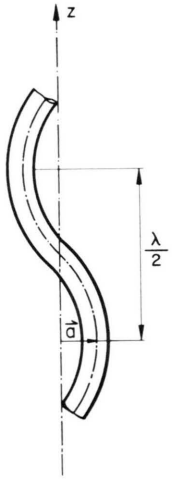

Fig. 2. Helically deformed arc column. Demonstration of the deflection a and the helix pitch λ.

different modes as performed in Eq. (1) it is possible here to build up arbitrary arc axis forms by use of Eq. (7) and the Fourier theorem. The case of a sinusoidal deflection will later be seen to be particularily useful. It can be derived from Eq. (7) by substituting $a_y = 0$.

2.3.2. Integral Momentum Balance

The integral momentum balance for the perturbation is as follows:

$$\int \mathbf{T}^*\,\mathrm{d}\mathbf{f} + \int \boldsymbol{\tau}^*\mathrm{d}\mathbf{f} - \int p^*\,\mathrm{d}\mathbf{f} - \int (\varrho\,\boldsymbol{v}\,\boldsymbol{v}_{\mathrm{MI}})^*\,\mathrm{d}\mathbf{f} = 0\,. \tag{9}$$

The integration is carried out over the arc surface generated by the boundary isotherm per unit arc length. In the formation of momentum flux density (last term) the relative velocity, $\boldsymbol{v}_{\mathrm{MI}}$, of the material with respect to the isotherm in question must therefore be substituted.

The individual terms have the following meaning:

$$\int \mathbf{T}^*\,\mathrm{d}\mathbf{f} = \boldsymbol{F}_{\mathrm{m}}^* \tag{10}$$

is the magnetic force per unit length, $\mathbf{T}^*$ being the perturbation part of the magnetic pressure tensor.

$$\int \boldsymbol{\tau}^*\,\mathrm{d}\mathbf{f} = \boldsymbol{F}_{\mathrm{v}}^* \tag{11}$$

is the force due to viscous friction per unit length, $\boldsymbol{\tau}^*$ the perturbation part of the shear stress tensor.

$$-\int p^*\,\mathrm{d}\mathbf{f} = \boldsymbol{F}_{\mathrm{p}}^* \tag{12}$$

is the pressure force, and includes all influences which arise from the inertia of the cold gas surrounding the electric arc.

In Eq. (9) the acceleration of the plasma has been neglected. This effect is always small by comparison with the term (12) on account of the low density in the plasma compared to the density of the cold gas.

The last term in the equation represents the convective momentum transport,

$$-\int (\varrho\,\boldsymbol{v}\cdot\boldsymbol{e}_1\,\boldsymbol{v}_{\mathrm{MI}})^*\,\mathrm{d}\mathbf{f} = \boldsymbol{F}_{\mathrm{c}}^*\,. \tag{13}$$

It can be further transformed. For the integrand

$$(\varrho\,\boldsymbol{v}\cdot\boldsymbol{e}_1\,\boldsymbol{v}_{\mathrm{MI}})^* = \varrho^0\,\boldsymbol{v}_{\mathrm{MI}}^0\cdot\boldsymbol{e}_1\,\boldsymbol{v}_{\mathrm{MI}}^* + \varrho^0\,\boldsymbol{v}^*\cdot\boldsymbol{e}_1\,\boldsymbol{v}_{\mathrm{MI}}^0 + \varrho^*\,\boldsymbol{v}_{\mathrm{MI}}^0\cdot\boldsymbol{e}_1\,\boldsymbol{v}_{\mathrm{MI}}^0 \tag{14}$$

where we made use of $\boldsymbol{v}^0 = \boldsymbol{v}_{\mathrm{MI}}^0$.

From Eq. (14) it can be seen that this convective term arises only when, in the undeflected arc, a flow is produced which penetrates the arc column. At first a theory will be developed without this sort of flow effect. This influence is discussed in a separate Section (3.3).

Therefore, with the help of the definitions (10–12) it is possible to rewrite Eq. (9) in the form

$$\boldsymbol{F}_{\mathrm{m}}^* + \boldsymbol{F}_{\mathrm{v}}^* + \boldsymbol{F}_{\mathrm{p}}^* = 0\,. \tag{15}$$

2.3.3. Average velocity of the Arc Relative to the Material due to Isotherm Movements

It has been possible to simplify the expression for momentum balance by means of the introduction of integral values. It should similarily be possible to obtain suitable integral values for the energy equation.

As has been shown in [5, 6] the energy equation can be transformed in such a manner that only the difference, $\boldsymbol{v}_{\mathrm{MI}}^*$, between the material velocity $\boldsymbol{v}^*$ and the isotherm velocity $\boldsymbol{v}_{\mathrm{I}}^*$ appears.

Corresponding to the definition for the position of the boundary isotherm, Eq. (6), the definition for the isotherm velocity in direction $\boldsymbol{e}_1$ is introduced.

$$\boldsymbol{v}_{\mathrm{I}}^* = -\boldsymbol{e}_1 [(\partial T^*/\partial t)_R/(\partial T^0/\partial r)_R] . \quad (16)$$

Here $\boldsymbol{v}_{\mathrm{I}}^*$, as discussed above, is identical with $\dot{\boldsymbol{a}}$.

In order to give an integral description of the results we make use of the relative velocity between the isotherm and the corresponding component of the flow velocity, averaged over the boundary isotherm.

$$\langle \boldsymbol{v}_{\mathrm{MI}}^* \rangle = \langle \boldsymbol{v}^* \rangle - \langle \boldsymbol{v}_{\mathrm{I}}^* \rangle \quad (17)$$

where

$$\langle \boldsymbol{v}^* \rangle = \frac{\boldsymbol{e}_1}{2\pi} \int_0^{2\pi} \boldsymbol{e}_1 \cdot \boldsymbol{v}^* (r = R, \varphi) \, \mathrm{d}\varphi . \quad (18)$$

2.4. Derivation of the Stability Equation by Means of the Integral Values

From the basic elements of the stability theory briefly mentioned in (2.2) together with general properties resulting from the linearity of the differential equations it is possible to derive certain functional dependences of the integral values.

The resultant flow resistance $\boldsymbol{F}_{\mathrm{v}}^* + \boldsymbol{F}_{\mathrm{p}}^*$ can be represented as (see [7]) linear functions of the perturbation velocity and acceleration

$$\boldsymbol{F}_{\mathrm{v}}^* + \boldsymbol{F}_{\mathrm{p}}^* = -f_1(X_1, \ldots, X_j) \langle \boldsymbol{v}^* \rangle - f_2(X_1, \ldots, X_j) \langle \dot{\boldsymbol{v}}^* \rangle ; \quad (19)$$

f_1 depends only on the friction, while f_2 has parts dependent on both friction and inertia.

For $\boldsymbol{F}_{\mathrm{m}}^*$

$$\boldsymbol{F}_{\mathrm{m}}^* = f_3(X_1, \ldots, X_j) \boldsymbol{a} . \quad (20)$$

Solution of the energy equation gives an eigenvalue for $\langle \boldsymbol{v}_{\mathrm{MI}}^* \rangle$ (see [8]). Furthermore $\langle \boldsymbol{v}_{\mathrm{MI}}^* \rangle$ must be proportional to a since the production term in the linearised energy equation is also proportional to a.

$$\langle \boldsymbol{v}_{\mathrm{MI}}^* \rangle = f_4(X_1, \ldots, X_j) \boldsymbol{a} . \quad (21)$$

Substituting Eqs. (19) and (20) in Eq. (15), replacing $\langle \boldsymbol{v}^* \rangle$ by $\langle \boldsymbol{v}_{\mathrm{MI}}^* \rangle + \dot{\boldsymbol{a}}$ [Eq. (17)] and substituting for $\langle \boldsymbol{v}_{\mathrm{MI}}^* \rangle$ from Eq. (21) produces an ordinary differential equation of the second order for the arc deflection a.

$$\alpha \ddot{a} + \beta \dot{a} + \gamma a = 0 \quad (22)$$

where α, β, γ are functions of f_i and therefore also of the system parameters $X_1, \ldots, X_j$.

$$\alpha = f_2; \quad \beta = f_2 f_4 + f_1; \quad \gamma = f_1 f_4 - f_3 . \quad (23)$$

The solution of Eq. (22) can be represented in the form

$$a(t) = a e^{\lambda t} \quad (24)$$

whereby the function $\lambda(X_1, \ldots, X_j)$ corresponding to Eq. (3) follows, from Eq. (22), with the statement (24)

$$\lambda = (\beta/2\alpha) [-1 \overset{+}{(-)} \sqrt{1 - 4\alpha\gamma/\beta^2}] \quad (25)$$

thus proving consistency with the statement (7).

The advantage of Eq. (22) with respect to the general procedure described in 2.2. is that the influences of the individual physical effects on the stability are directly recognisable.

As a result of (23) and (24) it is now possible to make the following general statements.

1. By means of Eqs. (23) and (25) it is easy to show that λ is always real. This means that below the stability boundary curve there always exist exponential decaying perturbations, while above the curve there is exponential growth. The boundary represents a stationary deflected condition ($\lambda = 0$).
2. The stability boundary curve is produced when $\gamma = 0$, or when

   $$f_1 f_4 = f_3 . \quad (26)$$

   This relationship allows the important statement that for stability the combined effects of friction (f_1) and isotherm movement (f_4) must be in equilibrium with that of the magnetic force (f_3). This statement can be interpreted as follows. The electromagnetically induced momentum in the deflected arc column can only be transported outwards by means of friction, since convective transport through the arc was excluded [see Equation (14)]. Friction is however only effective in the case of finite flow velocities. In order to compensate for this basically electro-magnetically induced residual flow it is therefore necessary to include the effect of isotherm movement.
3. In addition to the stability criterion given by Eq. (26), the convective stabilisation described in [3] is also possible if the arc remains in the observation region for a time which is small by

comparison with the time constant for the growth of the instability, as defined in Equation (25).

3. Discussion of the Stability Equation by Means of Dimensional Analysis

With the exception of numerical factors, which can only the found by means of an exact solution, it is possible, in many cases, to determine the relationships in the Eqs. (19), (20) and (21) by means of simple dimensional analysis considerations. It is then possible to carry out a very general discussion of the stability equation.

3.1. Free Burning Arc

The first type of arc to be discussed is one whose column is located at some distance from the boundary walls (e. g. a wall stabilised arc with very large wall radius, a non stationary growing electric arc, or an axially blown electric arc). This discussion is therefore particularily simple because the geometry is determined by only one parameter, i. e. the arc radius.

In agreement with the principles of dimensional analysis the integral values derived above are represented as the product of a group of dimensional values and a numerical factor z. It is then convenient to include the dependence of the wavelength in the numerical factor z.

On derivation of the correct dimensional factors an illustrative physical interpretation is taken as the starting point.

3.1.1. Magnetic Force

From [3] the magnetic force per unit length is

$$F_m^* = \mu_0 j^2 R^2 a z_1 \tag{27}$$

whereby z is known in this case:

$$z_1 = \pi \Phi(y) . \tag{28}$$

$\Phi(y)$ gives the wavelength dependence of the magnetic force: $y = R/b$. This function is represented in Figure 3. The magnetic force exhibits maximum at $y = 0.6$.

In the case where an axial magnetic field, B_0, is superimposed it is necessary to add an additional term to the magnetic force. From the statement (7) for the arc column is derived

$$F_{mB}^* = B_0 I a/b = B_0 I y a/R \tag{29}$$

per unit length. This force must be added to (27). Depending on the size of the magnetic field, B_0, either the self induced field effect (27) or the external field effect predominates. It is to be noted that both effects have a different wavelength dependence.

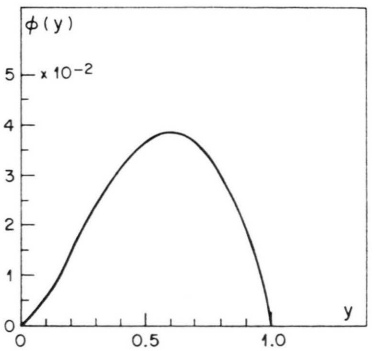

Fig. 3. Dependence of the self-induced magnetic force on $y = R/b$, $b = \lambda/2\pi$.

3.1.2. Movement of the Arc Column due to Isotherm Movement

3.1.2.1. Non Symmetrical Heating

A curved arc, with radius of curvature ϱ^*, exhibits an increased field strength on the concave side. For small radii

$$\Delta E/E = 2 R/\varrho^* . \tag{30}$$

The increased field strength on the concave side leads to increased heating there, which causes a corresponding increase of the energy transport term into the cold gas. As a result of this there is an increase in the relative velocity between mass and isotherm, or, more briefly, an increased isotherm movement $\langle \boldsymbol{v}_{MI}^* \rangle_E$.

In order to calculate $\langle \boldsymbol{v}_{MI}^* \rangle_E$ the energy balance is drawn up. The additional Joule heating $I \Delta E$ is required in order to bring that gas flowing perpendicularily to the arc to the enthalpy of the electric arc:

$$(\varrho h)_B \langle v_{MI}^* \rangle_E R \sim I \Delta E \tag{31}$$

where ϱh has been replaced by its value in the arc $(\varrho h)_B$. Thereby the cold gas enthalpy was defined as zero.

From Eq. (7) $\qquad \varrho^* = b^2/a \tag{32}$

and therefore, from (32), (30) and (31)

$$\langle v_{MI}^* \rangle_E \sim \frac{I E}{(\varrho h)_B} \frac{a}{b^2} \tag{33}$$

which can be written as

$$\langle v_{\mathrm{MI}}^{*}\rangle_E = \frac{I E}{(\varrho h)_B}\,\frac{a}{R^2}\,z_2\,, \tag{34}$$

$$z_2 = c_2\, y^2\,. \tag{35}$$

z_2 is, as has been explained above, the numerical factor which represents the special solution. The y dependence of this numerical factor, as given in (35) is, however, known.

3.1.2.2.Non Symmetrical Heat Flow

In the undisturbed arc the conducted Joule power $I E$ flows off in a purely radial direction as a heat flow W_r. With the deformation (7) of the arc column there emerges an axial component of $\boldsymbol{W}$:

$$W_z^{*} = W_r\, a/b\,. \tag{36}$$

Without additional effects W_z^{*} would, in the time δt, lead to an axially symmetric condition. In order to do this the heat flux W_z^{*} would be used to remove the arc volume of magnitude $a\,b\,R$ over the area $b\,R$.

$$(\varrho h)_B/\delta t \sim W_r^{*}\,. \tag{37}$$

To the build up of the asymmetry in the time δt there corresponds an isotherm velocity:

$$\langle v_{\mathrm{MI}}^{*}\rangle_W = a/\delta t\,. \tag{38}$$

Eqs. (36), (37) and (38) give, finally

$$\langle v_{\mathrm{MI}}^{*}\rangle_W = \frac{I E}{(\varrho h)_B}\,\frac{a}{R^2}\,z_3\,, \tag{39}$$

$$z_3 = c_3\, y\,. \tag{40}$$

and it can be seen that the same parameter dependences are derived as in Eq. (34). Only the wavelength dependence is different for the two effects.

In the following $\langle v_{\mathrm{MI}}^{*}\rangle_E$ and $\langle v_{\mathrm{MI}}^{*}\rangle_W$ are combined

$$\langle v_{\mathrm{MI}}^{*}\rangle = \frac{I E}{(\varrho h)_B}\,\frac{a}{R^2}\,z_4 \tag{41}$$

where

$$z_4 = z_2 + z_3\,. \tag{42}$$

3.1.3. Flow Resistance

3.1.3.1. Inertia of the Surrounding Cold Gas

In the event of an accelerating movement of the arc column, cold gas must also be accelerated. In this manner reaction builds up and appears as forces acting on the arc column (e. g. [3]). The same thing happens if the acceleration of the cold gas is brought about by $\langle v_{\mathrm{MI}}^{*}\rangle$. v^{*} on the arc boundary is the decisive term in the linear approximation regardless of how it is produced.

Continuing the dimensional analysis

$$F_{\mathrm{p}}^{*} = -R^2\,\varrho\,\langle \dot{\boldsymbol{v}}^{*}\rangle\, z_5\,. \tag{43}$$

As a special case the inertial resistance of a cylindrical obstacle follows from (43). The pitch dependence for the case of a helix has already been discussed in [3]. It is very weak and can be neglected in the present consideration.

3.1.3.2. Frictional Force

Since R is the only scale of length it follows immediately from dimensional considerations

$$F_{\mathrm{v}}^{*} = -\eta\,\langle v^{*}\rangle\, z_6\,. \tag{44}$$

This case also gives, as a special case, the frictional force on a cylinder, and the wavelength dependence can, to a first approximation, also be neglected.

3.1.4. Discussion of Stability Behaviour

3.1.4.1. Stability Equations

By means of the Eqs. (27), (41), (43) and (44) it is now possible, with the exception of numerical values, to find values for the function $f_1 - f_4$ in Equations (19) – (21). It is therefore possible to derive the coefficients in the stability equations

$$\alpha = R^2\,\varrho\, z_5\,, \tag{45}$$

$$\beta = \eta\, z_6 + \frac{\varrho\, I E}{(\varrho h)_B}\, z_4\, z_5\,, \tag{46}$$

$$\gamma = \eta\,\frac{I E}{(\varrho h)_B\, R^2}\, z_4\, z_6 - \mu_0\, j^2\, R^2\, z_1\,. \tag{47}$$

3.1.4.2. Stability Boundary Curve

As has already been derived in 2.4, the stability boundary curve is found by putting $\gamma = 0$. From Eq. (47)

$$\frac{\mu_0\, j^2\, R^2 (\varrho h)_B\, R^2}{\eta\, I E} = \frac{z_4\, z_6}{z_1}\,. \tag{48}$$

We introduce the following definitions

$$j\, R^2\, \pi = I\,, \tag{49}$$

$$j = \sigma\, E\,, \tag{50}$$

$$\sigma\, R^2\, \pi = G \tag{51}$$

where $G = I/E$ is the conductance of the arc column per unit length. From Eq. (48) it therefore follows that

$$\frac{\mu_0 (\varrho h)_B G}{\eta} = \frac{z_4 z_6 \pi^2}{z_1} \tag{52}$$

which can be written as in [2], in the form:

$$M k = M k_{cr} * \tag{53}$$

where

$$M k = \mu_0 (\varrho h)_B G/\eta , \tag{54}$$

$$M k_{cr} = z_4 z_6 \pi^2/z_1 . \tag{55}$$

The stable, helical deflected arc accordingly appears as a marginary case of stability when the dimensionless value $M k$ reaches the critical value $M k_{cr}$, which is determined by the boundary condition. $M k$ agrees with the form found in [2]. By means of the derivations carried out here the occurrence of this dimensionless value is easily recognised. The numerator arises from the magnetic force and the denominator from the product of the friction and isotherm velocity.

As will be shown in the next section the arc is unstable when $M k > M k_{cr}$. As the most important property of the arc the conductance G is found in the numerator of $M k$. This relationship explains the experimentally observed fact that high current arcs are less stable than low current ones, since high current arcs have a field strength which is comparable with, or even lower than, that of low current arcs. The conductance is therefore substantially higher. On going from a 10 A-arc to a 1000 A-arc the dimensionless constant then runs through at least two orders of magnitude.

The wavelength dependence of the stability criterion is contained in $M k_{cr}$.

The selfinduced magnetic force is wavelength dependent, as is the isotherm velocity in which two components are superimposed.

From (28), (35) and (40)

$$M k_{cr} = (c_2 y^2 + c_3 y)/\pi \Phi(y) . \tag{56}$$

In an experiment that wavelength will result which yields the smallest value of $M k_{cr}$. Depending on the size of the constant the corresponding value of y lies between $y = 0$, which gives for $c_3 = 0$ the position of the minimum, and $y = 0.34$ which, for $c_2 = 0$, gives the minimum of $M k_{cr}$.

* after Maecker.

The result of [1] is therefore generalised beyond the case of the wall stabilised arc.

In the present work it is also possible to determine immediately a corresponding stability criterion for the case where the external magnetic field predominates. In this case the Eq. (29) must be used in the derivation rather than (27). The stability criterion is then as follows:

$$(\varrho h)_B B_0 E/\eta = z_4 z_6/y . \tag{57}$$

In this case the fieldstrength of the arc emerges as the characteristic value in the numerator next to B_0. It can be seen that arcs with higher fieldstrengths are more sensitive to axial magnetic fields than those with lower field strength under similar conditions.

3.1.4.3. Behaviour in the Region of the Stability Boundary

In the region of the stability boundary it is possible to develop the root expression for small γ from Equation (25). This gives, for the growth rate:

$$\lambda = -\gamma/\beta . \tag{58}$$

γ can be expressed in term of $M k$ and $M k_{cr}$, giving finally

$$\lambda = \frac{\eta I E}{(\varrho h)_B R^2} \frac{z_1}{\pi^2} \frac{1}{\beta} (M k - M k_{cr}) . \tag{59}$$

The result of this formula, as mentioned above, is:

when $M k > M k_{cr}$ the arc is unstable $(\lambda > 0)$,

when $M k < M k_{cr}$ the arc is stable $(\lambda < 0)$.

A further consequence of Eq. (59) is that in the region of the stability boundary both the growth and decay rates are proportional to $(M k - M k_{cr})$. The physical values, which determine the proportionality factor, also follow from (59).

3.1.4.4. Growth Rate in the Unstable Region

In the event that $M k \gg M k_{cr}$ it is also possible to further simplify Equation (25). Under the square root sign the 1 can be neglected by comparison with the term $4 \alpha \gamma/\beta^2$. This gives directly

$$\lambda = \sqrt{-\gamma/\alpha} . \tag{60}$$

In this case γ is determined exclusively by the magnetic force. This gives

$$\lambda = j \sqrt{\frac{\mu_0}{\varrho} \frac{z_1}{z_5}} . \tag{61}$$

This result has already been derived in [3]. In this case $z_1/z_2 = F(y)$ was also calculated. Since z_5 is practically wavelength independent the largest growth rate is produced when the magnetic force is at a maximum, and this takes place, as is seen in Fig. 3 where $y = 0.6$ or $\lambda/D \approx 5$.

At large distances from the stability boundary the magnetic force and the inertial resistance of the cold gas determine both the growth rate and the wavelength dependence of the instability.

Taking this boundary case as a starting point those effects which can reduce the growth rate on approach to the stability boundary will now be discussed.

As has been shown above, in the region of the stability boundary, friction and isotherm movement are equally important. It will now be shown that between this case, and the boundary case (61) there exists a region where the growth rate is determined from the inertial force and the isotherm movement. This region is represented by

$$M k > M k_{cr} \quad \text{and} \quad 4\alpha\gamma < \beta^2 . \qquad (62)$$

Under these conditions γ is exclusively determined through the magnetic force while the growth rate is already strongly reduced with respect to (61) because of β. In β the effects of isotherm movement generally predominate [see Eq. (46)]. Therefore, for the region (62), the above expression is proven.

It is important for experiments that in the event of an instability the isotherm movement is effective in both reducing the growth rate and increasing the wavelength, or reducing y. In that case the minimum of $M k_{er}$, which, when influenced solely by a magnetic field, lies in the region of 0.6 [Eq. (61)], shifts, under the influence of the isotherm movement in the region between $y = 0.34$ and $y = 0$ [see Equation (56)].

3.2. Influence of Walls in the Region of the Arc

Until now it has been assumed that the containing walls have been at a considerable distance and have not influenced the stability criterion. In the framework of the present discussion it is an easy matter to include a qualitative assessment of the effects of the walls.

3.2.1. Arcs in Circularily Cylindric Tubes

This is the case investigated by Mentel [1]. It will be quickly demonstrated here that the results derived from the present method are consistent with the rigorous solution.

The magnetic force [see Eq. (27)] and the isotherm velocity [see Eq. (41)] are purely column effects and are therefore to be considered unchanged in this case. In addition to the isotherm movement however there arises an effect due to the walls. Furthermore, the two flow resistance values F_p^* and F_v^* are influenced by the wall. Since only the stability criterion will be discussed here, F_p^* can be neglected.

3.2.1.1. Frictional Force with a Wall Stabilised Arc

The flow field, which is produced by the magnetic force, leads, as is shown in Fig. 4, to a double vortex which is closed along the gap, δ, between the wall and the arc. The result of this is that for the frictional force, R is no longer the only controlling dimension; δ is now also important. The case which is considered here is that in which the friction in this gap is the dominating effect. The shear stress on the arc surface due to friction in the gap amounts to

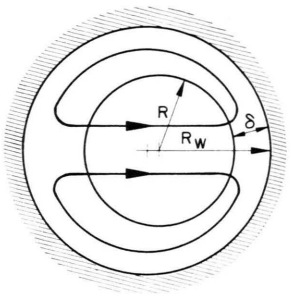

Fig. 4. Cross section of the arc column in a circular tube.

$$\tau^* = \eta v^*/\delta \qquad (63)$$

and the force on the complete arc can be found by integration over the arc surface, or by following the dimensional analysis given here.

$$F_v^* = -\eta \langle v^* \rangle (R/\delta) z_7 . \qquad (64)$$

3.2.1.2. Isotherm Movement due to Asymmetrical Energy Flow to the Wall

In addition to the disturbance of the heat flow due to the curvature of the arc, as calculated in 3.1.2.2., there is, in this case a disturbance of the heat flow in a radial direction, since the deflected arc is nearer to the wall. In the form of a linear approximation

$$W_r^* = W a/\delta . \qquad (65)$$

In a manner which is completely analogous to the procedure of 3.1.2.2. it is then possible to calculate an additional $\langle v^*_{MI} \rangle$

$$\langle v^*_{MI} \rangle = \frac{I E a}{(\varrho h)_B R^2} \frac{R}{\delta} z_8 . \qquad (66)$$

This expression is added to the term (41).

3.2.1.3. Discussion of the Stability Criterion

As was done in [2] the definition of $M k$ as given in Eq. (54) remains unchanged. The additional terms then appear in $M k_{cr}$,

$$M k_{cr} = [(R/\delta) z_7 \pi (c_2 y^2 + c_3 y + z_8 R/\delta)]/\Phi(y) \qquad (67)$$

where the y dependence of $M k_{cr}$ is explicitly given. It can be seen that the friction shows a dependence R/δ in $M k_{cr}$. The curve given in [2] corresponds exactly to this dependence.

The wavelength dependence consists of several superimposed effects. A result of [1], for a certain parameter range, is that the wavelength depends only on the tube radius. This follows from (67) for a certain relationship of the numerical factors c_2, c_3 and z_8. In a larger parameter range a dependence on the arc radius should appear according to Equation (67).

In addition to these remarks it is also to be noticed that with the above method Mentel's solution can easily be extended to include the region outside the neutral stability curve and also the case with an axial magnetic field.

3.2.2. Electric Arcs in Gaps Between Insulated Boundaries

This type of arc is of great practical significance. It shows the characteristics displayed in Figure 5.

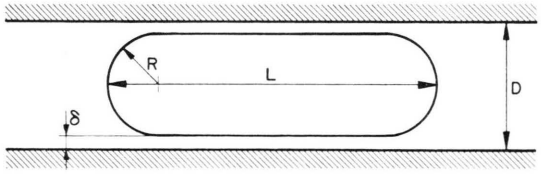

Fig. 5. Cross section of an arc in a gap.

Due to lateral limitation the arc takes on an oval form. It looses its heat by conduction through the gap δ to the wall.

Because of the lateral limitation only a sinusoidal instability is possible in a plane parallel to the plates. As a further consequence of this geometry certain exceptions occur for the stability determining effects derived above. They will be discussed in at least a qualitative manner.

3.2.2.1. Magnetic Force

In order to simplify the estimation of the magnetic force the oval arc cross section is considered to be composed of several circularly formed arcs. The total force is the sum of the individual forces. At the maximum of the sinusoidal instability the same formulas apply for the remainder as for the helix. This gives

$$F_m^* = (L/2R) \mu_0 j^2 R^2 a z_9 , \qquad (68)$$

where z_9 again contains the unchanged y dependence with respect to (28).

3.2.2.2. Thermal Velocity

On deriving the isotherm velocity due to asymmetrical heating corresponding to 3.1.2.1. the following change appears:

$$\Delta E/E = L/\varrho^* \qquad (69)$$

giving

$$\langle v^*_{MI} \rangle_E = \frac{I E}{(\varrho h)_B} \frac{a}{R^2} \frac{L}{R} z_{10} \qquad (70)$$

with

$$z_{10} = c_{10} c^2 . \qquad (71)$$

(39) and (40) on the other hand are unchanged.

3.2.2.3. Frictional Force

In the same way as was the case with the wall stabilised arc the friction at the edge of the arc is determined by the gap δ, thus:

$$F_v^* = -\eta \langle v^* \rangle (L/\delta) z_{11} . \qquad (72)$$

3.2.2.4. Pressure Force

Since the gas, on acceleration, can not expand laterally, but must be transported from regions with deflection towards the right to regions with deflection towards the left, the pressure force is wavelength dependent. On the assumption that a volume of size bR per unit length must be accelerated, it follows that

$$F_p^* = \varrho \langle v^* \rangle z_{12} \qquad (73)$$

where

$$z_{12} = c_{12}/y . \qquad (74)$$

3.2.2.5. Discussion of the Stability Equation and the Growth Rate

The value Mk is again constructed in a manner analogous to (54) only now

$$j = I/2RL, \tag{75}$$

$$G = \sigma 2RL, \tag{76}$$

$$Mk = (\varrho h)_B \mu_0 G/\eta \tag{77}$$

giving a value for Mk_{cr} of

$$Mk_{cr} = z_{11} \frac{[c_{10}(L/R)y^2 + c_3 y]}{\pi \Phi(y)} \frac{L}{\delta} \frac{L}{R}. \tag{78}$$

Equation (78) contains the following dependences:

(a) Because of the lateral walls the friction is increased and thereby the stability is improved in a manner similar to that occurring for a wall stabilised arc.

(b) Because of the variation of the circular form, as expressed in the relation L/R, the stability is also improved [factor L/R in Equation (78)].

Simultaneously, as a consequence, the isotherm movement due to asymmetrical heating is favoured with respect to the heat conduction term. In this way, for the case of large L/R, Mk_{cr} has a quadratic dependence on L/R. There is also a shift in wavelength, since, as has been mentioned above, the asymmetric heating, together with the magnetic force at $y = 0$, gives a minimum value of Mk_{cr}.

In the unstable region $Mk \gg Mk_{cr}$, where magnetic force and pressure force are in equilibrium, a change with respect to the free arc column is produced because of the y dependence of the pressure force as given in Equation (75). The dependence $y\varphi(y)$ has a maximum at $y = 0.71$, i. e. it results, in this case, in a small shift of y to $\lambda/D = 4.5$.

3.3. Influence of a Flow Field on the Stability of Electric Arcs

3.3.1. External Flow Field

An external flow field $\boldsymbol{v}^0$ around the electric arc also influences the coefficients in the integral values

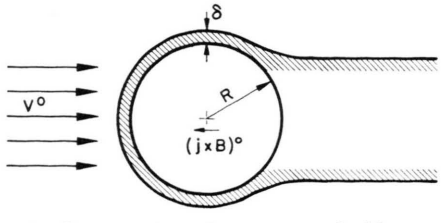

Fig. 6. Cross section of a transversely blown arc.

in a characteristic way. As an example of this the so-called transversely blown electric arc (see Fig. 6) is discussed in greater detail.

This type of arc is held stationary, with respect to a flow by means of a transverse magnetic field.

At the arc boundary a temperature and vorticity boundary layer of thickness δ is built up, the value of δ depending strongly on the flow velocity v^0.

Behind the electric arc is found a flow separation whose properties still remain largely unexamined.

A discussion of the stability properties of this type of arc is therefore restricted to some qualitative observations.

The effects associated purely with the column, i. e. the magnetic force [Eqs. (27) and (29)] and the thermal movement [Eq. (41)] are still valid.

As a further approximation it can be taken that the pressure force behaves according to Equation (43). So long as the flow around the body can be approximated by a potential flow, this is exact, because Eq. (43) also follows from a potential expression which can be superimposed on the undisturbed flow. In the present case there is an additional contribution arising from the wake behind the arc.

As was the case with the wall stabilised arc there appear however strong additional influences caused by the effects of the boundary layer on the thermal velocity and on the friction. For both effects the limit of the boundary layer represents, by definition, the boundary for frictional and heat conductive influences (although, strictly speaking, the two effects each have different boundary layer thicknesses).

For this reason a stabilisation factor R/δ is added to F_v^* as in Eq. (64) and to the thermal velocity v_{MI}^* is added a contribution corresponding to Eq. (66) having the dependence R/δ. The build up of the boundary layer has a stabilising effect corresponding to the remarks of 3.2.1.3.

It is however to be noted that in the case of the build up of a broad wake as indicated in Fig. 6, the boundary layer behind the arc cannot play a stabilising role. The electric arc will therefore first break out into this wake in a manner similar to an electric arc in a gap (3.2.2.).

3.3.2. Flow Through the Boundary Isotherm

When, even in the non-deflected initial condition, a material flow $\boldsymbol{v}_{MI}^0$ takes place through the bound-

ary isotherm, then it is necessary to consider the convective momentum transport of Equation (13).

The corresponding momentum flux density at the arc boundary is represented by Equation (14). The discussion is limited to the first term on the right hand side. This is proportional to $\langle v_{MI}^{*} \rangle$. It is therefore possible, together with Eq. (21), and in analogy with the derivation of 2.3.3., to write:

$$\boldsymbol{F}_c^{*} = f_5(X_1, \ldots, X_j) \langle \boldsymbol{v}_{MI}^{*} \rangle \tag{79}$$

which, together with Eq. (21) gives

$$\boldsymbol{F}_c^{*} = f_5 f_4 \boldsymbol{a} . \tag{80}$$

F_c^{*} therefore displays the same parameter dependence as F_m^{*}. Of the parameters (23) of the stability Eq. (22) only γ changes

$$\gamma = f_4(f_1 - f_5) - f_3 . \tag{81}$$

Since $\gamma = 0$ is the criterion for stability this also changes.

Since f_5 appears in addition to the coefficient of the friction f_1, it can be said that the convective momentum transport influences the stability in a manner analogous to the friction. Therefore:

When $f_5 > 0$ there is a destabilising influence,

when $f_5 < 0$ there is a stabilising influence.

Two examples of the qualitative consequences of this effect will now be examined more closely.

In the first example a source or a sink flow in the arc is considered. An example of an arc with a sink flow is described in [3].

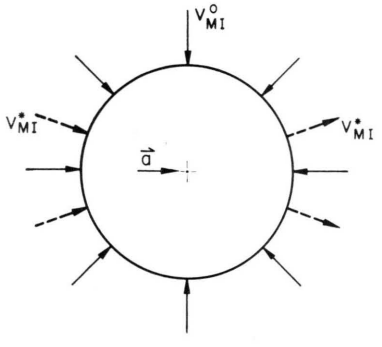

Fig. 7. Flow field at the boundary of a deflected arc with radial inflow v_{MI}^{0}.

With the help of Fig. 7 it is now easy to derive:

$$\boldsymbol{F}_c^{*} = \pm v_{MI}^{0} \varrho R \langle \boldsymbol{v}_{MI}^{*} \rangle z_{13} , \tag{81}$$

where + = Flow into the arc (sink), − = Flow out of the arc (source).

This permits the statement: A source flow was a stabilising effect while a sink flow has a destabilising effect.

In the region of the stability boundary

$$\langle v_{MI}^{*} \rangle \approx \langle v^{*} \rangle ,$$

and there it is possible to express simply the relative significance of the convective and frictional terms.

$$\frac{F_c^{*}}{F_v^{*}} \sim \frac{v_{MI}^{0} \varrho R}{\eta} = \mathrm{Re} . \tag{82}$$

The convective term therefore dominates the frictional term if the Reynold's number, which is based on the flow velocity through the boundary isotherm and the arc radius, is sufficiently large.

In the second example a flow transverse to the boundary isotherm is taken (see Fig. 8) and the

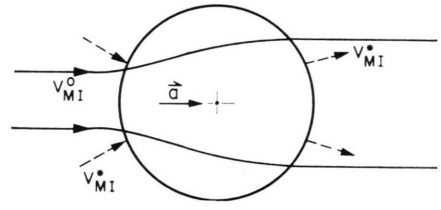

Fig. 8. Flow field of a convectively stabilized arc with a transverse flow v_{MI}^{0}.

case of a deflection in the direction of this transverse flow is considered. The signs of the contribution on both left and right are different in this case. Depending on which side predominates, there is either a stabilising or destabilising effect. Furthermore, in this case, the flow leads to an anisotropic behaviour. The deflections, in direction defined by the flow direction, are modified.

With the help of Fig. 8 a case is briefly discussed.

If the influence of the asymmetrical heating [Eq. (34)] predominates in v_{MI}^{*}, then v_{MI}^{*} is larger on the concave left side, and it predominates the left hand side, i. e. there is a destabilising effect. This can be easily imagined. Because of the increased inflow from the left additional momentum in the direction a is introduced into the arc. The deflections are increased. If the deflections are toward the left then the isotherm movement v_{MI}^{*} on the left hand side is impaired and it can introduce less positive x-momentum, which in this case would work reactively, into the arc.

4. Conclusions

In the present paper a formalism has been derived on the basis of rigorous stability theory with which it is possible to separately determine and judge the different physical effects which influence the stability of an electric arc. This approach has yielded valuable indications as to how these instabilities might be controlled experimentally.

The derivations represent an initial framework of considerations for different types of arc. The two previously known rigorous solutions are seen as special cases. The aims of future work will be to experimentally verify the various exhibited effects and to find, for one or other of the especially interesting cases, a rigorous solution of the equations.

Thanks are due to Dr. W. Schneider, Dr. L. S. Dzung, Dr. W. Hermann and Dr. L. Niemeyer for clarifying discussions.

[1] J. Mentel, Z. Naturforsch. **26 a**, 526 [1971].
[2] K. A. Ernst, J. Kopainsky, and J. Mentel, Z. Phys. **265**, 253 [1973].
[3] K. Ragaller, U. Kogelschatz, and W. R. Schneider, Z. Naturforsch. **28 a**, 1321 [1973].
[4] S. Chandrasekhar, Hydrodynamic and Hydromagnetic Stability, Oxford at the Clarendon Press, Oxford 1961.
[5] H. Maecker, Proc. IEEE **59**, 439 [1971].
[6] K. Ragaller, W. R. Schneider, and W. Hermann, Z. Angew. Math. Phys. **22**, 920 [1971].
[7] L. D. Landau and E. M. Lifshitz, Fluid Mechanics, § 24, Pergamon Press, Oxford 1959.
[8] W. Hermann and K. Ragaller, Proc. IX. Int. Conference on Phenomena in Ionized Gases, Bukarest 1969.